



Lennon, David, and Parker, Stewart F. (2014) Inelastic neutron scattering studies of methyl chloride synthesis over alumina. *Accounts of Chemical Research*, 47 (4). pp. 1220-1227. ISSN 0001-4842

Copyright © 2014 American Chemical Society

<http://eprints.gla.ac.uk/92961>

Deposited on: 05 August 2014

Enlighten – Research publications by members of the University of Glasgow_
<http://eprints.gla.ac.uk>

Inelastic Neutron Scattering Studies of Methyl Chloride Synthesis over Alumina

David Lennon[†] and Stewart F. Parker^{*‡}

[†]Department of Chemistry, University of Glasgow, Joseph Black Building, Glasgow G12 8QQ, U.K.

[‡]ISIS Facility, STFC Rutherford Appleton Laboratory, Chilton, Didcot, Oxon OX11 0QX, U.K.

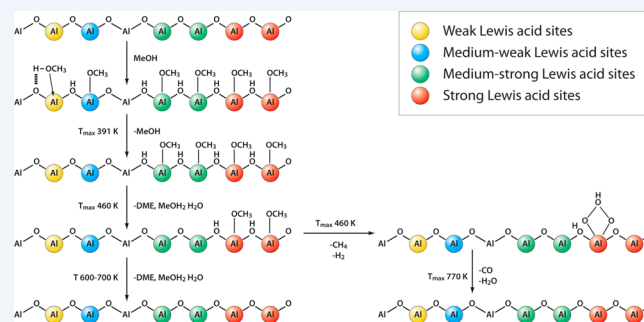
ABSTRACT: Not only is alumina the most widely used catalyst support material in the world, it is also an important catalyst in its own right. One major chemical process that uses alumina in this respect is the industrial production of methyl chloride. This is a large scale process (650 000 metric tons in 2010 in the United States), and a key feedstock in the production of silicones that are widely used as household sealants. In this Account, we show how, in partnership with conventional spectroscopic and reaction testing methods, inelastic neutron scattering (INS) spectroscopy can provide additional insight into the active sites present on the catalyst, as well as the intermediates present on the catalyst surface.

INS spectroscopy is a form of vibrational spectroscopy, where the spectral features are dominated by modes involving hydrogen. Because of this, most materials including alumina are largely transparent to neutrons. Advantageously, in this technique, the entire “mid-infrared”, 0–4000 cm^{-1} , range is accessible; there is no cut-off at $\sim 1400 \text{ cm}^{-1}$ as in infrared spectroscopy. It is also straightforward to distinguish fundamental modes from overtones and combinations.

A key parameter in the catalyst's activity is the surface acidity. In infrared spectroscopy of adsorbed pyridine, the shifts in the ring stretching modes are dependent on the strength of the acid site. However, there is a very limited spectral range available. We discuss how we can observe the low energy ring deformation modes of adsorbed pyridine by INS spectroscopy. These modes can undergo shifts that are as large as those seen with infrared spectroscopy, potentially enabling finer discrimination between acid sites.

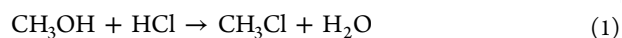
Surface hydroxyls play a key role in alumina catalysis, but in infrared spectroscopy, the presence of electrical anharmonicity complicates the interpretation of the O–H stretch region. In addition, the deformations lie below the infrared cut-off. Both of these limitations are irrelevant to INS spectroscopy, and all the modes are readily observable. When we add HCl to the catalyst surface, the acid causes changes in the spectra. We can then deduce both that the surface chlorination leads to enhanced Lewis acidity and that the hydroxyl group must be threefold coordinated.

When we react η -alumina with methanol, the catalyst forms a chemisorbed methoxy species. Infrared spectroscopy clearly shows its presence but also indicates the possible coexistence of a second species. Because of INS spectroscopy's ability to discriminate between fundamental modes and combinations, we were able to unambiguously show that there is a single intermediate present on the surface of the active catalyst. This work represents a clear example where an understanding of the chemistry at the molecular level can help rationalize improvements in a large scale industrial process with both financial and environmental benefits.



INTRODUCTION

Alumina is ubiquitous in heterogeneous catalysis, where it is used as an actual catalytic material or as a catalyst support material.¹ As a consequence of its ready availability, structural stability, and ability to be prepared in a variety of pore size distributions, alumina is the most widely used catalyst support material.² The interaction of methanol with alumina has been extensively studied for many years, not least because alumina is one of the components for the industrial methanol synthesis catalyst. However, the interaction of methanol with alumina is also important in the industrial scale manufacture of methyl chloride,³ where methanol and hydrogen chloride are combined over high surface area alumina catalysts, for example, γ -alumina:



Methyl chloride is a large scale commodity chemical: demand in the USA in 2010 was estimated to be 650 000 t. The compound is used in many processes, but the bulk is used for the production of methyl chlorosilanes, which are intermediates in the production of silicones.

In this Account, we show how, in partnership with conventional spectroscopic and reaction testing methods, inelastic neutron scattering (INS) spectroscopy⁴ can provide

Received: November 13, 2013

Published: February 28, 2014

additional insight into the active sites present on the catalyst and the intermediates present on the surface.

INS SPECTROSCOPY

Inelastic neutron scattering spectroscopy is a form of vibrational spectroscopy that is complementary to infrared and Raman spectroscopies. The key difference between vibrational neutron spectroscopy and infrared and Raman spectroscopies is that the neutron has mass, in contrast to a photon; thus an inelastic scattering event results in a significant transfer of *both* energy (ω , cm^{-1}) and momentum (Q , $|Q| = Q$, \AA^{-1}). The intensity, S , of an INS band is given by⁴

$$S(Q, n\omega_i) \propto \frac{(QU_i)^{2n}}{n!} \exp(-QU_{\text{Tot}}^2) \sigma \quad (2)$$

where ω_i is the i th mode at frequency ω , $n = 1$ for a fundamental, 2 for a first overtone or binary combination, 3 for a second overtone or ternary combination, etc., Q is the momentum transfer, U_i is the root-mean-square displacement of the atoms in the mode, and σ is the inelastic scattering cross section of the atom. The exponential term in eq 2 is a Debye–Waller factor, U_{Tot} is the total root-mean-square displacement of all the atoms in all the modes (both internal and external), and its magnitude is in part determined by the thermal motion of the molecule. This can be reduced by cooling the sample, so INS spectra are typically recorded below 30 K, as were all the spectra shown here. The cross section, σ , is both element- and isotope-dependent, and for ^1H , it is almost 2 orders of magnitude larger than for most other species. Further, since it is also the lightest isotope of the lightest element, it has the largest amplitude of vibration; these two factors combine so that while there are no selection rules for INS spectroscopy, there is a strong “propensity rule” such that in hydrogenous materials, modes that involve motion of hydrogen will dominate the spectrum.

In the work described here, two INS spectrometers at the ISIS Facility⁵ are used: TOSCA and MARI. These instruments are complementary, TOSCA has a fixed path through (Q, ω) space and provides good resolution in the 0–1600 cm^{-1} region, while MARI can observe both Q and ω independently and so provides a map of (Q, ω) space. It also enables observation of the 1600–4000 cm^{-1} region, unhindered by the electrical anharmonicity that complicates infrared spectroscopy in this region.

CHARACTERIZATION OF ACID SITES ON η -ALUMINA

Large scale hydrochlorination of methanol can be achieved over solid acid catalysts, with η -alumina being one such catalyst. The surface acidity of η -alumina was determined by a combination of infrared spectroscopy and volumetric and gravimetric adsorption experiments using pyridine as a probe molecule.⁶ The results are shown in Figure 1; four Lewis acid sites are detected: weak, medium-weak, medium-strong, and strong. All the sites have a coordinatively unsaturated aluminum ion present; however, the coordination number of this ion and its neighbors varies with the type of site, and an adjacent hydroxyl has a progressively lower coordination number as the acid strength increases, $3 \rightarrow 2 \rightarrow 1 \rightarrow 0$.

While infrared spectroscopy of the bands of adsorbed pyridine in the 1400–1650 cm^{-1} range and the corresponding changes in the O–H stretch region were the key technique to

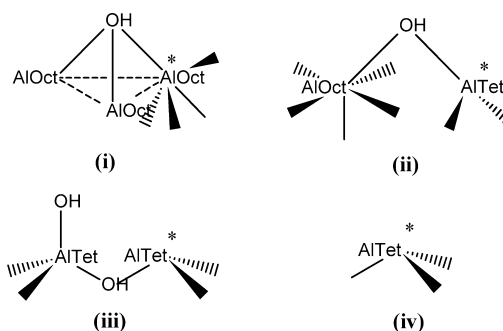


Figure 1. Schematic representations of the proposed acid sites of activated η -alumina: (i) the weak Lewis acid site, (ii) the medium-weak Lewis acid site, (iii) the medium-strong Lewis acid site, and (iv) the strong Lewis acid site. The asterisks indicate coordinative unsaturation. Reproduced from ref 6 with permission. Copyright 2005 American Chemical Society.

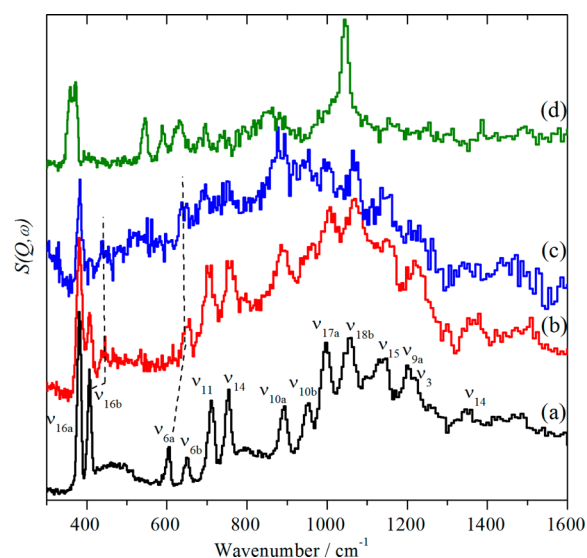


Figure 2. INS spectra recorded at 20 K of (a) solid pyridine and (b) background subtracted η - Al_2O_3 + 896 μmol of pyridine g^{-1} , (c) the chemisorbed pyridine spectrum after heating the adsorbed overlayer to 473 K in flowing helium for 30 min, and (d) pyridinium chloride. Adapted from ref 6 with permission. Copyright 2005 American Chemical Society.

characterize the different sites, the same sample was also investigated by INS spectroscopy. The aim was to investigate whether some of the low frequency modes of adsorbed pyridine, which are inaccessible via infrared spectroscopy, could be used to probe local acidity functions. Figure 2a shows the INS spectrum of pyridine, where distinct bands below the ~ 1400 cm^{-1} infrared cutoff of alumina are evident. The spectrum of a pyridine overlayer (896 μmol of pyridine g^{-1}) on activated η -alumina is shown in Figure 2b. With reference to the volumetric adsorption isotherm, this amount of pyridine retention by the catalyst involves a substantial physisorption component, so unsurprisingly, the overlayer spectrum is similar to the reference spectrum. However, the $\nu_{6a}(A_1)$ mode at 605 cm^{-1} is absent in the spectrum of the adsorbed overlayer. Additionally, a weak but distinct feature at 440 cm^{-1} is also evident in Figure 2b. The overlayer was then warmed to 473 K in a continuous stream of helium, and the spectrum was recorded (Figure 2c). From previous work,⁶ it is known that this treatment will eliminate physisorbed pyridine, the

Table 1. Assignment of the Spectra of Pyridine Adsorbed at the Strong Lewis Acid Site on η -Alumina

mode and description	pyridine, cm^{-1}			adsorbed pyridine, cm^{-1}	
	infrared, Raman ^a	INS (solid)	symmetry	infrared (δ) ^b	INS (δ) ^b
ν_{16a} ring torsion	374	382	A_2		382 (0)
ν_{16b} ring torsion	406	406	B_1		439 (+33)
ν_{6a} in-plane ring deformation	605	604	A_1		637 (+33)
ν_{6b} in-plane ring deformation	653	650	B_2		649 (-1)
ν_{11} out-of-plane C–H bend + ring torsion	701	712	B_1		694 (-18)
ν_4 out-of-plane C–H bend + ring torsion	748	754	B_1		752 (-2)
ν_{10a} out-of-plane C–H bend	884	891	A_2		880 (-11)
ν_{10b} out-of-plane C–H bend	942	953	B_1		946 (-7)
ν_{17a} out-of-plane C–H bend	984		A_2		
ν_1 ring breathing	991	997	A_1		998 (+1)
ν_5 out-of-plane C–H bend	1007		B_1		
ν_{12} ring stretch	1030		A_1		
ν_{18b} ring stretch + in-plane C–H bend	1068	1056	B_2		1068 (+12)
ν_{18a} ring stretch + in-plane C–H bend	1072		A_1		
ν_{15} ring stretch + in-plane C–H bend	1146	1137	B_2		1154 (+17)
ν_{9a} ring stretch + in-plane C–H bend	1216	1201	A_1		
ν_3 ring stretch + in-plane C–H bend	1227	1219	B_2		1223 (+4)
ν_{14} ring stretch + in-plane C–H bend	1355	1350	B_2		
ν_{19b} ring stretch	1437		B_2	1449 (+12)	
ν_{19a} ring stretch	1482		A_1	1492 (+10)	
ν_{8b} ring stretch + in-plane C–H bend	1574		B_2	1577 (+3)	
ν_{8a} ring stretch + in-plane C–H bend	1581		A_1	1623 (+42)	

^aData from ref 8 for the liquid. ^b $\delta = [(\text{adsorbed pyridine}) - (\text{pure pyridine})]$.

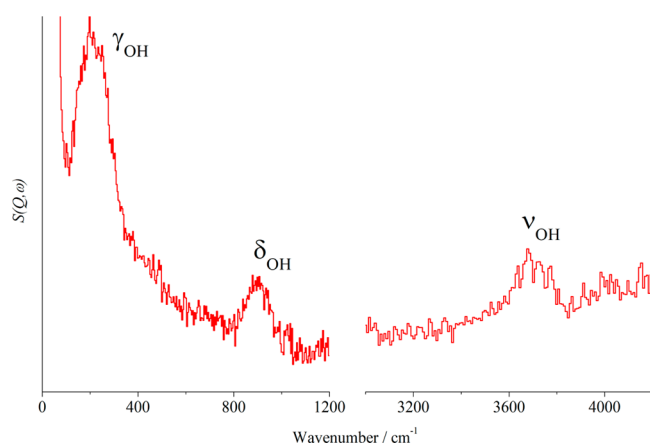


Figure 3. INS spectra of the η -alumina catalyst after activation at 623 K recorded at 20 K using the MARI spectrometer with an incident energy of (a) 4840 cm^{-1} ($3000\text{--}4200 \text{ cm}^{-1}$) and (b) 1290 cm^{-1} ($50\text{--}1200 \text{ cm}^{-1}$). Reproduced from ref 9 with permission of Elsevier, copyright 2006.

chemisorbed pyridine residing in all of the weak Lewis acid sites, and $\sim 35\%$ of that in the medium Lewis acid sites. Thus, Figure 2c corresponds to the INS spectrum of pyridine residing in predominantly medium and strong Lewis acid sites.

The spectrum of adsorbed pyridine is usually discussed just in terms of the bands in the $1400\text{--}1650 \text{ cm}^{-1}$ region. However, there is extensive literature on the vibrational spectra of coordination complexes of pyridine,⁷ and the extended spectral range that INS enables means that these additional modes are accessible. Table 1 compares the transition energies of liquid pyridine⁸ with those of pyridine chemisorbed in the strong site. The $\nu_{19b}(B_2)$, $\nu_{19a}(A_1)$, and $\nu_{8a}(A_1)$ modes are diagnostic of the strength of the interaction, particularly the $\nu_{8a}(A_1)$ mode, which undergoes a large shift. However, it is apparent that the lower

energy modes are potentially equally diagnostic because the shifts for $\nu_{16b}(B_1)$ and $\nu_{6a}(A_1)$ modes are almost as large as that seen for the $\nu_{8a}(A_1)$ mode.

Finally, the absence in Figure 2b,c of any obvious relative intensity enhancement of the $\nu_{18b}(B_2)$ in-plane C–H deformation about 1060 cm^{-1} confirms the absence of substantial Brønsted acidity for this catalyst because this feature dominates the INS spectrum of the pyridinium ion, Figure 2d. Collectively, these results demonstrate that the INS spectrum of an adsorbed probe molecule offers some potential in evaluating surface acidity. It is complementary to the infrared spectrum, and the two very different methodologies provide the full vibrational spectrum of the chemisorbed base.

Figure 3 shows the INS spectrum⁹ of η -alumina after activation by heating in flowing helium at 623 K for 150 min recorded using the MARI spectrometer operating at incident energies (E_i) of 4840 and 1290 cm^{-1} . Spectral resolution on this instrument is related to the incident energy selected ($\sim 2\% E_i$), so recording spectra over two energy ranges means reasonable resolution can be maintained over a wider spectral range than that obtainable at a single energy.¹⁰ A broad feature that spans $3600\text{--}3800 \text{ cm}^{-1}$ with a maximum at 3676 cm^{-1} is assigned to the O–H stretch of hydroxyl groups present at the alumina surface. The peak at 905 cm^{-1} is assigned to the deformation mode of surface hydroxyl groups. This mode is generic to all hydroxyls. However, for the terminal hydroxyl group associated with the medium-strong site as depicted in Figure 1c, this feature represents an in-plane hydroxyl deformation, δ_{OH} . The intense feature at $\sim 200 \text{ cm}^{-1}$ is assigned to the out-of-plane deformation of surface hydroxyl groups, γ_{OH} . This mode approximates to a torsional motion of the hydroxyl group. Such modes normally yield intense features in INS spectra. It is noted that the δ_{OH} and γ_{OH} modes of alumina are not normally observable by infrared spectroscopy.

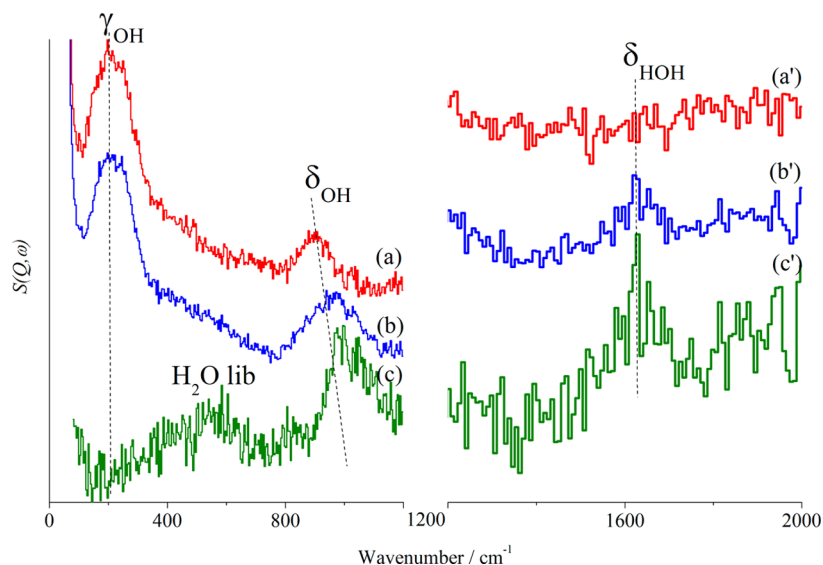


Figure 4. INS spectra recorded at 20 K using the MARI spectrometer with incident energies of 1280 cm^{-1} (normal text) and 2420 cm^{-1} (primed text) for (a, a') the η -alumina background, (b, b') a saturated chemisorbed overlayer of HCl on η -alumina (prepared at 300 K), and (c, c') the difference spectrum (these are $\times 2$ ordinate expanded with respect to the parent spectra). Adapted from ref 9 with permission of Elsevier, copyright 2006.

■ THE INTERACTION OF HYDROGEN CHLORIDE WITH η -ALUMINA

The INS spectra of the catalyst before and after exposure to gaseous HCl is shown in Figure 4a,b, and the difference is

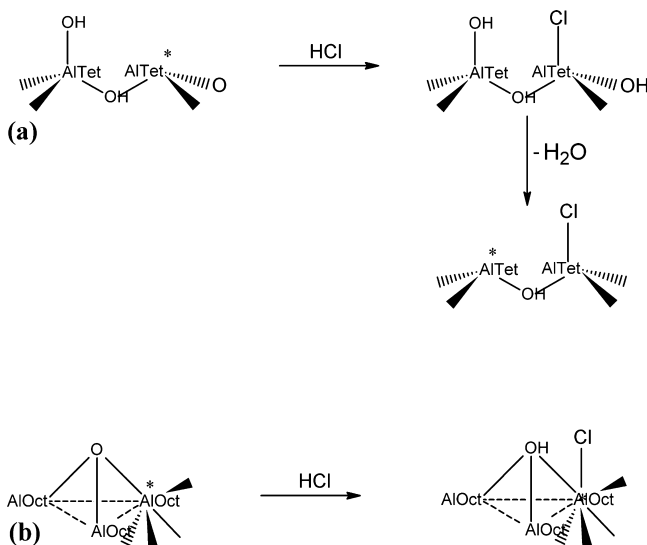
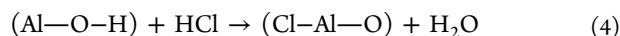
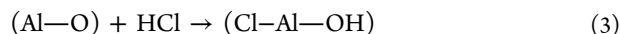


Figure 5. A schematic representation of (a) the adsorption of HCl at a medium-strong Lewis acid site and the effect of subsequent H_2O loss and (b) HCl dissociatively adsorbed at a coordinatively unsaturated aluminum site with the adjacent oxygen atom exhibiting 3-fold coordination. The asterisks indicate coordinative unsaturation. Reproduced from ref 9 with permission of Elsevier, copyright 2006.

shown in Figure 4c. Figure 4a is assigned as δ_{OH} at 900 cm^{-1} and γ_{OH} at 210 cm^{-1} . After reaction with HCl, Figure 4b,b', there is some attenuation of the γ_{OH} feature at 210 cm^{-1} , and changes are apparent in the δ_{OH} region, particularly around 1000 cm^{-1} , indicating a shift to higher wavenumber for this feature, and a band appears at 1630 cm^{-1} . The background subtracted spectrum, Figure 4c,c', demonstrates these pertur-

bations to the hydroxyl signals more clearly. The negative inflection about 180–210 cm^{-1} confirms the loss of hydroxyl groups contributing to the γ_{OH} mode, and the δ_{OH} mode shows an increase in intensity at 1000 cm^{-1} , which is resolvable into two peaks at 990 and 1050 cm^{-1} . A broad feature at $\sim 550 \text{ cm}^{-1}$ is also discernible; this is assigned to the librational modes of water, and the 1630 cm^{-1} peak is assigned to the water scissors mode.

The changes are consistent with the known chemistry of HCl on alumina:



Equation 3 involves the dissociation of HCl onto aluminum oxygen pairs forming new hydroxyl groups and Al–Cl species. Equation 4 is similar in that it also proceeds via dissociative adsorption of the HCl but with a hydroxyl exchange mechanism, where chlorine replaces a surface hydroxyl group coordinated to an aluminum ion, and generation of water. Infrared spectroscopy of this system had shown that the medium-strong site (Figure 1c) was interacting with the HCl as shown in Figure 5a. The INS spectrum is consistent with this process because it shows loss of the γ_{OH} mode at 210 cm^{-1} and formation of water (librational modes at $\sim 550 \text{ cm}^{-1}$). There must also be loss of intensity in the δ_{OH} region, and this is seen as the negative-going feature at $\sim 900 \text{ cm}^{-1}$. Interestingly, such a transformation leads to the regeneration of an active site, and due to the increased electronegativity of the chlorine relative to a hydroxyl group, the newly generated Lewis acid site will be more acidic than the original. This suggests that chlorination via HCl should lead to enhanced Lewis acidity.

Temperature-programmed reaction studies⁹ had shown that all four Lewis acid sites interacted with HCl. Figure 4c shows that there is generation of new hydroxyl sites as well as the loss of the terminal hydroxyls. Since only one split band is observed, this means that it must be 3-fold coordinated hydroxyl, because both terminal and 2-fold bridging hydroxyls will have an in-plane bending mode near 900 cm^{-1} and an out-of-plane bend at

500 cm^{-1} or less, and this is not observed. Figure 5b shows a process that would be consistent with the observations: the site approximates the weak Lewis acid site, Figure 1a, although in this instance the bridging oxygen atom is not bonded to a hydrogen. The hydroxyl group exhibits pseudo- C_{3v} symmetry for which the deformation mode is doubly degenerate; however, under the pseudo- C_{3v} symmetry encountered at this site, the degeneracy will be partially lifted, leading to two peaks as observed.

A feature of neutron spectrometers such as MARI, is that the measured neutron intensity, $S(Q,\omega)$, is a function of both energy (ω , cm^{-1}) and momentum (Q , \AA^{-1}).^{4,10} This capability can be exploited to determine whether a particular vibrational feature is a fundamental mode ($n = 1$) or whether it corresponds to a higher order transition ($n \geq 2$).¹¹ In the present instance, the maximum of the $S(Q,\omega)$ versus Q plot ($dS(Q,\omega)/dQ \approx 0$) for the feature at $\sim 900 \text{ cm}^{-1}$ occurs at relatively low Q ($\sim 8 \text{ \AA}^{-1}$), confirming that this is a fundamental, whereas an $n \geq 2$ transition would be expected at $Q \geq 11 \text{ \AA}^{-1}$. (The precise value at which the maximum in $S(Q,\omega)$ occurs is system dependent; however, it is typically 5–8 \AA^{-1} , and an $n = 2$ transition will occur at a value that is $\sqrt{2}$ larger).

■ THE INTERACTION OF METHANOL WITH η -ALUMINA

Figure 6 shows a comparison of the INS spectra of solid methanol, chemisorbed methoxy, and a model compound,

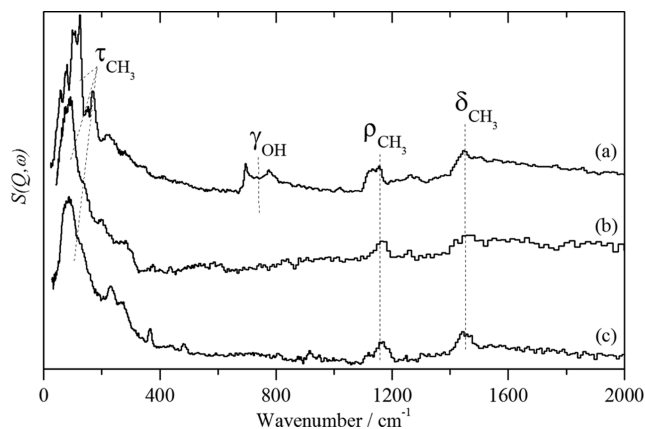


Figure 6. INS spectra recorded at 20 K using TOSCA of (a) methanol, (b) background subtracted spectrum of a saturated chemisorbed overlayer of methoxy on η -alumina ($1.12 \text{ mmol CH}_3\text{OH g}^{-1}$) prepared at 300 K, and (c) $\text{Al}(\text{OCH}_3)_3$. Reproduced from ref 12 by permission of the PCCP Owner Societies, copyright 2005.

$\text{Al}(\text{OCH}_3)_3$.¹² In all three spectra, the intense structured feature below 400 cm^{-1} is due largely to the methyl torsion. For methanol, Figure 6a, the complex band shape at $690\text{--}780 \text{ cm}^{-1}$ is assigned to the out-of-plane O–H bend (γ_{OH}). In the low temperature α -phase of methanol,¹³ there are four molecules in the unit cell; thus factor group splitting is observed. The two other major features, at 1150 and 1450 cm^{-1} , are assigned to the methyl rock (ρ_{CH_3}) and a mode resulting from the overlap of methyl deformation modes (δ_{CH_3}) and the in plane O–H bend, respectively. Figure 6b shows the INS spectrum resulting from the reaction of methanol with η -alumina at 300 K. It is clearly different from that of solid methanol, as indicated by the

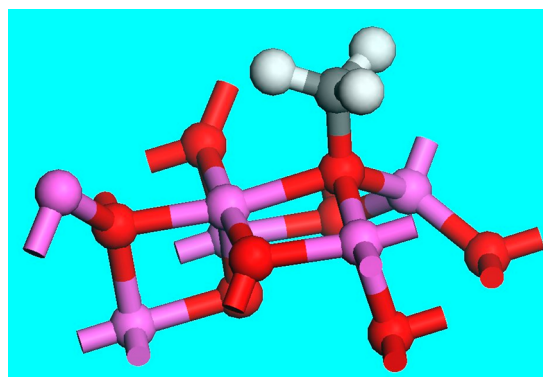


Figure 7. Energy minimized structure for methoxy on η -alumina(110). Purple = aluminum; red = oxygen; gray = carbon; white = hydrogen. Reproduced from ref 12 by permission of the PCCP Owner Societies, copyright 2005.

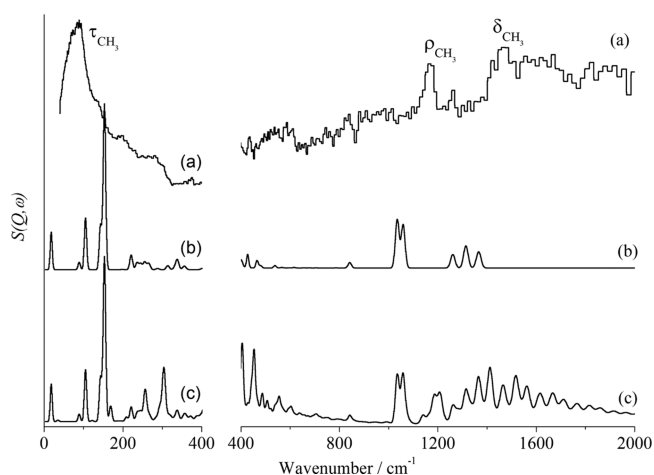


Figure 8. (a) Background subtracted spectrum of a saturated chemisorbed overlayer of methoxy on η -alumina ($1.12 \text{ mmol CH}_3\text{OH g}^{-1}$) prepared at 300 K and recorded at 20 K, showing the methyl torsion (τ), rock (ρ), and bending (δ) modes. Calculated INS spectrum for methoxy on η -alumina(110), (b) fundamentals ($n = 1$) only and (c) with inclusion of overtones and combinations up to $n = 10$. The right-hand side is ordinate expanded $\times 3$ for panel a and $\times 5$ for panels b and c relative to the left-hand side. Reproduced from ref 12 by permission of the PCCP Owner Societies, copyright 2005.

absence of the out-of-plane O–H bend at $690\text{--}780 \text{ cm}^{-1}$ and strongly resembles the spectrum of the model compound $\text{Al}(\text{OCH}_3)_3$, Figure 6c. The relatively weak spectrum is indicative of the low density of active sites present on the η -alumina surface. The spectrum is characterized by the intense CH_3 torsion at 84 cm^{-1} (τ_{CH_3}), the CH_3 rock at 1170 cm^{-1} and the CH_3 deformation modes at 1460 cm^{-1} and is assigned to chemisorbed methoxy species, formed from the dissociative adsorption of methanol. The differences between spectra b and c in Figure 6 are the result of the three interacting methoxy groups in $\text{Al}(\text{OCH}_3)_3$, whereas the low density of active sites on the η -alumina surface means that the surface methoxy groups do not interact with one another.

Periodic density functional theory calculations of methoxy on the (110) η -alumina surface confirm the assignment to adsorbed methoxy. The calculations are based on the structure shown in Figure 7, which is an idealized structure with all the oxygen atoms in tetrahedral sites and the aluminum present only in tetrahedral and octahedral sites. This simplifies the

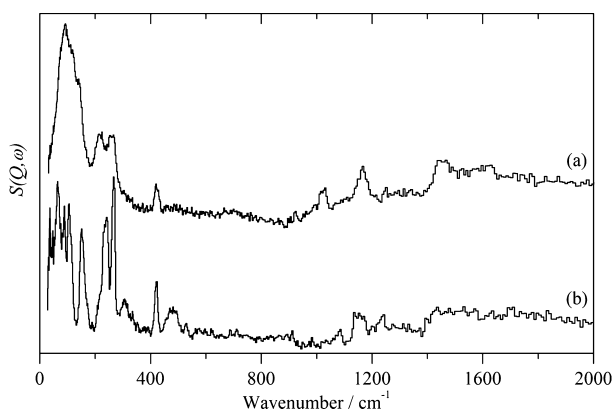


Figure 9. INS spectra recorded at 20 K using TOSCA of (a) background subtracted spectrum of η -alumina dosed with excess methanol ($1.57 \text{ mmol CH}_3\text{OH g}^{-1}$) at 300 K, isolated and warmed to 473 K for 15 min, and (b) dimethyl ether. Reproduced from ref 12 by permission of the PCCP Owner Societies, copyright 2005.

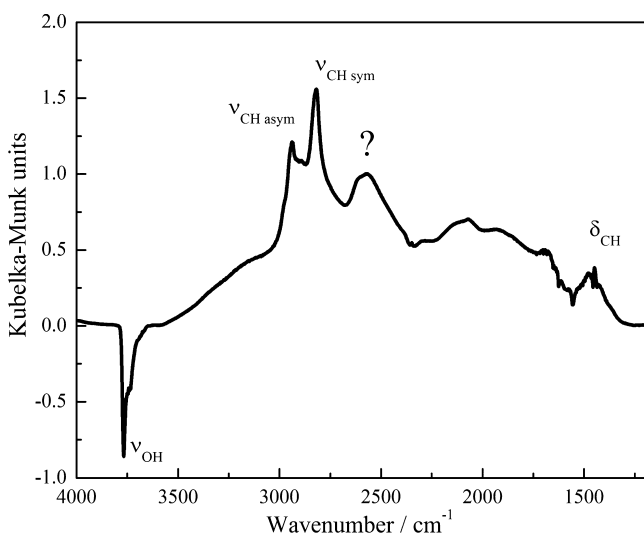


Figure 10. The background subtracted diffuse reflectance infrared spectrum of methoxy on η -alumina at 300 K showing the loss of hydroxyls (ν_{OH}), the appearance of the methoxy bands ($\nu_{\text{CH-asym}}$, $\nu_{\text{CH-sym}}$, δ_{CH}), and the unassigned feature (?). Reproduced from ref 12 by permission of the PCCP Owner Societies, copyright 2005.

calculations significantly. The energy minimized structure for methoxy on η -alumina(110) has the C–H bonds in an “eclipsed” conformation relative to the Al–O bonds; the alternative “staggered” conformation did not produce an energy minimum. The O–CH₃ distance is 1.485 Å, and the C–H bond distances are 1.105, 1.109, and 1.112 Å. Figure 8 shows a comparison of the observed INS spectrum (Figure 8a) to that calculated with just the fundamentals, that is, $n = 1$ only (Figure 8b), and with inclusion of overtones and combinations up to $n = 10$. (Figure 8c). The overall pattern is reproduced, and inspection of the modes confirms the assignments given earlier. The methyl torsion and the Al–O–C bends, together with their overtones and combinations, are responsible for the intense feature near 100 cm^{-1} . The alumina lattice modes contribute weakly at $200\text{--}400 \text{ cm}^{-1}$, where the mode results in motion of the methyl group and the internal methyl modes are at their usual energies. The O–C stretch is calculated at 843 cm^{-1} . This results in little proton motion and is barely

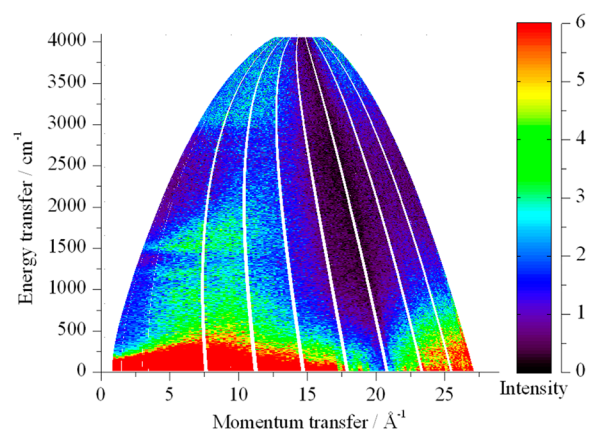


Figure 11. INS spectrum of a saturated chemisorbed overlayer of methoxy on η -alumina prepared at 300 K and recorded using the MARI spectrometer at 20 K with an incident energy of 4034 cm^{-1} . Some shadowing of the detectors by the catalyst cell is present as shown by the dark area at $Q > 15 \text{ \AA}^{-1}$. Reproduced from ref 12 by permission of the PCCP Owner Societies, copyright 2005.

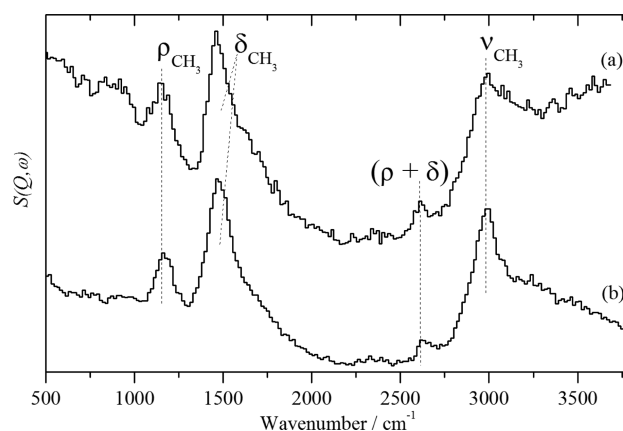
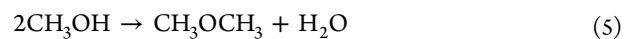


Figure 12. INS spectra recorded using the MARI spectrometer with an incident energy of 4034 cm^{-1} for (a) methoxy on η -alumina and (b) the model compound $\text{Al}(\text{OCH}_3)_3$. Both spectra are from the low momentum transfer region, $0 \leq Q \leq 15 \text{ \AA}^{-1}$; spectrum a is from the data shown in Figure 11. Reproduced from ref 12 by permission of the PCCP Owner Societies, copyright 2005.

detectable in Figure 8a. The weak feature at 1264 cm^{-1} is a combination between the methyl rock and the torsion.

One of the problems associated with methyl chloride synthesis, eq 1, is that dimethyl ether, CH_3OCH_3 , is formed as an unwanted byproduct, eq 5:



Infrared spectroscopy¹⁴ and temperature-programmed reaction studies¹⁵ show that dimethyl ether is formed over the same temperature range as methyl chloride, implying that the same reactive methoxy species are involved in both processes. Figure 9a shows the INS spectrum obtained after adsorption of excess methanol on η -alumina followed by subsequent heating to 473 K in an isolated cell. A reference spectrum of solid dimethyl ether is presented in Figure 9b. In the region $1100\text{--}1600 \text{ cm}^{-1}$, Figure 9a is broadly similar to that of adsorbed methoxy, Figure 6b, since both methanol and dimethyl ether share common structural motifs. However, distinct bands at 218, 260, and 420 cm^{-1} are present in Figure 9a but absent in Figure 6b. By comparison to the reference spectrum, Figure 9b, these bands

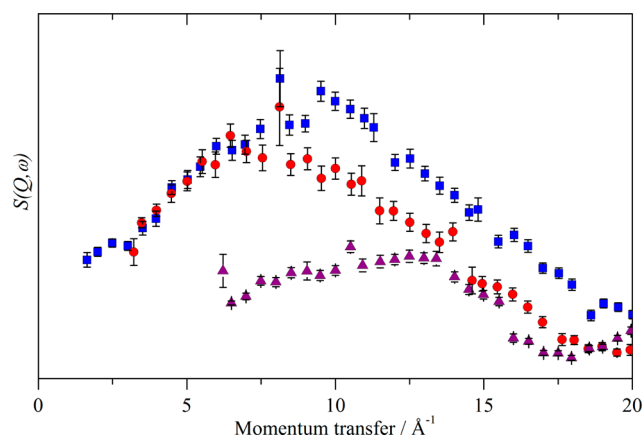


Figure 13. The momentum transfer dependence of the modes at 1186 (C–H rock, blue squares), 1456 (C–H deformations, red circles), and 2630 cm^{-1} (purple triangles) for the chemisorbed methoxy sample. Reproduced from ref 12 by permission of the PCCP Owner Societies, copyright 2005.

are associated with dimethyl ether. These modes are respectively assigned as $\nu_{11}(A_2)$ out-of-phase methyl torsion, $\nu_{21}(B_2)$ in-phase methyl torsion, and $\nu_7(A_1)$ C–O–C bend of dimethyl ether and confirmed by DFT calculations. The band at 480 cm^{-1} in Figure 9b is assigned to a combination mode of the C–O–C bend and the lattice mode at 62 cm^{-1} (480 $\text{cm}^{-1} \approx 417 + 62 \text{ cm}^{-1}$). Its absence in Figure 9a indicates that the dimethyl ether is disordered on the surface, which is confirmed by the unstructured appearance of the external modes in the 0–200 cm^{-1} region of Figure 9a, in comparison to the sharp, well-defined modes present in the same region in Figure 9b. Thus, Figure 9a can be explained in terms of formation of dimethyl ether from the dimerization of surface methoxy species.

The diffuse reflectance infrared spectrum of a chemisorbed layer of methoxy on η -alumina is shown in Figure 10. All of the features are readily assigned to methoxy, except the band at $\sim 2600 \text{ cm}^{-1}$. Two possible assignments were to either methoxy or a second surface species.

The operating principle of TOSCA means that modes at $>1600 \text{ cm}^{-1}$ are usually very difficult to observe, in contrast with MARI where these are straightforward.¹⁰ Figure 11 presents the neutron scattering intensity as a function of energy transfer and momentum transfer for the chemisorbed overlayer.

The need for a large sample and consequently its container has resulted in some shadowing of the detectors, such that the momentum transfer range available is restricted. Summing only the detectors in the range 0–15 \AA^{-1} for the saturated chemisorbed overlayer of methoxy on η -alumina and also for $\text{Al}(\text{OCH}_3)_3$ generates the spectra shown in Figure 12. The C–H stretch at 2950 cm^{-1} (ν_{CH_3}), methyl deformations at 1460 cm^{-1} (δ_{CH_3}), and methyl rock at 1165 cm^{-1} (ρ_{CH_3}) are apparent; however, a weak feature at $\sim 2600 \text{ cm}^{-1}$ is also present in both spectra, as seen in the infrared spectrum, Figure 10. The transition energy would suggest that it is a combination mode of the rock + deformations ($1156 + 1459 = 2615 \text{ cm}^{-1}$), and this is confirmed by the momentum transfer dependence of the mode. Figure 13 shows the Q -dependence of the modes at 1186, 1456, and 2630 cm^{-1} for the chemisorbed methoxy sample. The poor signal-to-noise ratio reflects the small amount of sample present, and the shadowing of the detectors restricts the useful Q -range; however, it is clear that the fundamentals, 1186 cm^{-1} (C–H rock) and 1456 cm^{-1} (C–H deformations), peak at a lower Q than the 2630 cm^{-1} mode, showing that this latter feature is indeed a higher order process. Applying the same method to the $\text{Al}(\text{OCH}_3)_3$ data confirms this conclusion.

CONCLUSIONS

The chemistry of methanol on η -alumina is summarized in Figure 14. This represents the results from many techniques in addition to INS spectroscopy, and it is reiterated that a multitechnique approach is crucial to successful investigations.

Nonetheless, the advantages of INS spectroscopy have proven to be crucial in developing our understanding of this industrially important process. In particular, the specificity toward hydrogen and the access to modes that lie below the alumina cutoff in the infrared spectrum at $\sim 1100 \text{ cm}^{-1}$, which include the Al–O–H deformation modes, the methoxy methyl rock, and torsion, were essential in order to characterize the surface chemistry. While infrared spectroscopy of adsorbed pyridine will undoubtedly continue to be a key method for the determination of surface acidity, the shifts for the $\nu_{16b}(B_1)$ and $\nu_{6a}(A_1)$ modes at 406 and 605 cm^{-1} are almost as large as that seen for the $\nu_{8a}(A_1)$ mode at 1582 cm^{-1} . Thus, there is the potential to provide complementary information.

All techniques have disadvantages as well as advantages, and INS spectroscopy is no exception. The three most serious are

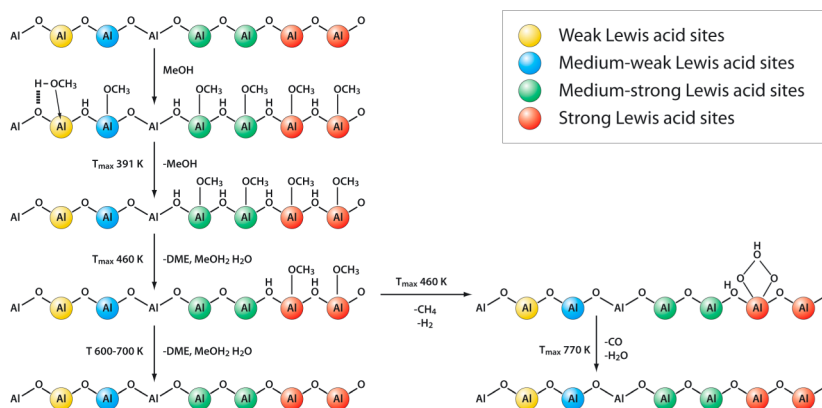


Figure 14. A schematic representation for the site-selective interaction of methanol with η -alumina. The geometric arrangement of the different surface sites has no direct significance, although their coloring specifically reflects the surface acidity of the four distinct sites. Reproduced from ref 14 with permission. Copyright 2005 American Chemical Society.

limited access to facilities, sample size, and the need to measure at 30 K. INS spectroscopy requires the use of central facilities and there are a limited number of these, with the ISIS Facility⁵ (Chilton, U.K.) and the Institut Laue Langevin¹⁶ (Grenoble, France) being the leading facilities in Europe. The access has recently improved with the opening of the state-of-the-art facilities SNS¹⁷ (Knoxville, TN, USA) and J-PARC¹⁸ (Tokai, Japan), which have almost doubled the number of INS spectrometers available. INS spectroscopy is a relatively insensitive technique, and studies of catalysts typically require 10–50 g of sample. For new materials this can be a problem; however, for industrial catalysts, the averaging inherent in a large sample means that concerns about representative sampling are greatly reduced. Generally, samples are prepared at or above room temperature and then cooled to the measurement temperature, so, in essence, we are taking snapshots along the reaction profile. However, recent work has demonstrated that with careful experimental design and an appropriate choice¹⁰ of spectrometer type, it is feasible to study reactions under *in operando* conditions at room temperature.¹⁹

The spectroscopic evidence demonstrates that there is only one intermediate present on the η -alumina surface and that is methoxy. As a result of initiatives at the industrial complex, it proved possible to modify the surface properties of the catalyst so as to drastically reduce the amount of dimethyl ether produced and the attendant cost of recycling it back to methanol. This a clear example where an understanding of the chemistry at the molecular level has helped rationalize improvements in a large scale industrial process with both financial and environmental benefits.

AUTHOR INFORMATION

Corresponding Author

*E-mail: stewart.parker@stfc.ac.uk

Notes

The authors declare no competing financial interest.

Biographies

David Lennon received a Ph.D. in physical chemistry from the University of East Anglia (Norwich, U.K.) in 1989. After postdoctoral research at The University of Texas at Austin, The University of Western Australia, and the University of East Anglia, he joined the University of Glasgow as the ICI Lecturer in Heterogeneous Catalysis in 1996. He was promoted to Senior Lecturer in 2000 and to Reader in 2007. His interests are in surface chemistry and heterogeneous catalysis, at both the gas/solid and liquid/solid interfaces, and he has extensive collaborations with industry throughout Europe. He is a member of the recently established UK Catalysis Hub based at Harwell.

Stewart F. Parker received a Ph.D. in physical chemistry from the University of California at Santa Barbara in 1983. After postdoctoral research at the University of East Anglia, he joined the Analytical Division of the British Petroleum Research Centre at Sunbury-on-Thames in 1985. In 1993, he joined the ISIS Facility at the Rutherford Appleton Laboratory as an instrument scientist. He is currently the ISIS Scientist for Catalysis Research, and his interests are the application of vibrational, particularly inelastic neutron scattering, spectroscopy to energy related topics, including catalysis, hydrogen storage, and charge storage materials. He is a member of the recently established UK Catalysis Hub based at Harwell.

ACKNOWLEDGMENTS

The authors thank the STFC Rutherford Appleton Laboratory for access to neutron beam facilities. Computing resources were provided by STFC's e-Science facility. The EPSRC is thanked for support for the development of the INS catalyst cells and gas rig (Grant EP/E028861/1). John Winfield (University of Glasgow), Chris Dudman, and Peter Jones (Ineos ChloroVinyls) are thanked for helpful discussions. David Lundie and Alastair McInroy are thanked for technical assistance.

REFERENCES

- (1) Weissmehl, K.; Arpe, H.-J. *Industrial Organic Chemistry*, 3rd ed.; VCH: Weinheim, Germany, 1997.
- (2) Farrauto, R. J.; Bartholomew, C. H. *Fundamentals of Industrial Catalytic Processes*; Blackie: London, 1997; p 60.
- (3) Satterfield, C. N. *Heterogeneous Catalysis in Industrial Practice*, 2nd ed.; Krieger Publishing: Malabar, FL, 1996.
- (4) Mitchell, P. C. H.; Parker, S. F.; Ramirez-Cuesta, A. J.; Tomkinson, J. *Vibrational Spectroscopy with Neutrons with Applications in Chemistry, Biology, Materials Science and Catalysis*; World Scientific: Singapore, 2004.
- (5) <http://www.isis.stfc.ac.uk/>.
- (6) Lundie, D. T.; McInroy, A. R.; Marshall, R.; Winfield, J. M.; Mitchell, C.; Dudman, C. C.; Jones, P.; Parker, S. F.; Lennon, D. An Improved Description of the Surface Acidity of eta-Alumina. *J. Phys. Chem. B* **2005**, *109*, 11592–11601.
- (7) Thornton, D. A. Metal Complexes of Pyridine: Infrared and Raman Spectra with Particular Reference to Isotopic Labelling Studies. *Coord. Chem. Rev.* **1990**, *104*, 251–295.
- (8) Partal Ureña, F.; Fernández Gómez, M.; López González, J. J.; Martínez Torres, E. A New Insight into the Vibrational Analysis of Pyridine. *Spectrochim. Acta, Part A* **2003**, *59*, 2815–2839.
- (9) McInroy, A. R.; Lundie, D. T.; Winfield, J. M.; Dudman, C. C.; Jones, P.; Parker, S. F.; Lennon, D. A Temperature-Programmed Desorption, Infrared and Inelastic Neutron Scattering Spectroscopic Study of the Interaction of Hydrogen Chloride with η -Alumina. *Catal. Today* **2006**, *114*, 403–411.
- (10) Parker, S. F.; Lennon, D.; Albers, P. W. Vibrational Spectroscopy with Neutrons – a Review of New Directions. *Appl. Spectrosc.* **2011**, *65*, 1325–1341.
- (11) Parker, S. F.; Bennington, S. M.; Aufferman, G.; Bronger, W.; Herman, H.; Williams, K. P. J.; Smith, T. Inelastic Neutron Scattering, Raman Spectroscopy and Periodic-DFT Studies of Rb_2PtD_6 and Rb_2PtD_6 . *J. Am. Chem. Soc.* **2003**, *125*, 11656.
- (12) McInroy, A. R.; Lundie, D. T.; Winfield, J. M.; Dudman, C.; Jones, P.; Parker, S. F.; Taylor, J. W.; Lennon, D. An Infrared and Inelastic Neutron Scattering Spectroscopic Investigation on the Interaction of η -Alumina and Methanol. *Phys. Chem. Chem. Phys.* **2005**, *7*, 3093–3101.
- (13) Torrie, B. H.; Weng, S.-X.; Powell, B. M. Structure of the α -Phase of Solid Methanol. *Mol. Phys.* **1989**, *67*, 575.
- (14) McInroy, A. R.; Lundie, D. T.; Winfield, J. M.; Dudman, C. C.; Jones, P.; Lennon, D. The Application of Diffuse Reflectance Infrared Spectroscopy and Temperature-Programmed Desorption To Investigate the Interaction of Methanol on η -Alumina. *Langmuir* **2005**, *21*, 11092–11098.
- (15) McInroy, A. R.; Lundie, D. T.; Winfield, J. M.; Dudman, C. C.; Jones, P.; Lennon, D. Improved Atom Efficiency via an Appreciation of the Surface Activity of Alumina Catalysts: Methyl Chloride Synthesis. *Appl. Catal., B* **2007**, *70*, 606–610.
- (16) <http://www.il.eu>.
- (17) <http://neutrons.ornl.gov/>.
- (18) <http://j-parc.jp/en/message.html>.
- (19) Parker, S. F. The Role of Hydroxyl Groups in Low Temperature Carbon Monoxide Oxidation. *Chem. Commun.* **2011**, *47*, 1998–1990.